Proceedings World Geothermal Congress 2005
Antalya, Turkey, 24-29 April 2005

Modeling of the Dachny Site Mutnovsky Geothermal Field (Kamchatka, Russia) in Connection with the Problem of Steam Supply for 50 MWe Power Plant

Alexey V. Kiryukhin

Institute of Volcanology Far East Branch of Russian AS Piip- 9, Petropavlovsk-Kamchatsky, 683006

E-mail: avk2@kcs.iks.ru

Keywords: Geothermal, reservoir, modeling, Mutnovsky.

ABSTRACT

The Mutnovsky geothermal field modeling study (TOUGH2) previously made by the author (Kiryukhin, 1992, 1996, 2002) has shown that total steam production of the wells existing in 1991 will yield not less than 44 MWe x 20 years. In October 2002 Mutnovsky 50 MWe PP was put into operation in Dachny site. The problem of steam supply to Mutnovsky 50 MWe PP (Dachny) trigged the new reservoir model study. Current conceptual model of the Dachny site based on mapping of active fracture zones, circulation losses and production zones distribution data, gas and fluid chemistry data, secondary minerals distributions, recent results of drilling and geothermal analog data reveals "single fault" nature of reservoir (the Main production zone in Dachny site strikes north-north-east and dip east-east-south at the angle 60^o. The old model (1992, 1996, 2002) has been revised and the new one based on "well-by-well" generated mesh (A-Mesh grid generator) strongly related to the particular wells and production zones has been used. The following data are used for the new model calibration: (1) pre-exploitation flowtests from wells E4, 016, 26, 029W and 24, (2) additional wells A1 – A4 drilling data, (3) pressure monitoring data (well 012) and (4) exploitation wells E4, 016, 26, 029W, A2, E5 (2002-2003 year) output data. Modeling results show that total steam production of the operating wells (E4, 016, 26, 029W, E5) will decline from 60-70 kg/s to 30 kg/s during the period of 10 year exploitation due to overload of the north part of the Main production zone. Modeling of the various exploitation scenarios show necessity of drilling of the seven additional wells in the south-eastern part of the Dachny site to maintain 50 MWe PP.

1. INTRODUCTION

The previous numerical model of the Mutnovsky geothermal field (1992, 1996) was designed to understand heat and mass transfer processes in geothermal reservoir as a whole, and to forecast possible exploitation scenarios. This model consisting of 500 elements 500 x 500 x 500 m^3 each with total volume of 5 x 5 x 2.5 km^3 was used to forecast 20 year period of exploitation based on existing wells and it shown 44 MWe as a minimum yield of the field. Next time this model was used by WestJec (Japan) company to do feasibility study of the Mutnovsky PP. After AO "Geotherm" having put this PP into operation in October 2002 30-35% steam supply shortage was found. Since that reservoir modeling was applied as an instrument for optimal design of the exploitation load in relation to the particular production zones was revealed and loaded in the field. Geothermal reservoir is represented as a combination of two reservoirs: A-reservoir and B-reservoir. A-reservoir corresponds to the "single fault type" Main production zone. B-reservoir includes elements corresponding to diorite intrusion contact permeability zones. In total 24 existing wells, 39 additional interior elements and 12 boundary (inactive) elements (B-elements) are specified in the model, the coupled wellbore flow in this model was realized based on TOUGH2V2.0 (K.Pruess, 1999) option.

2. CONCEPTUAL HYDROGEOLOGICAL MODEL OF THE MUTNOVSKY GEOTHERMAL FIELD

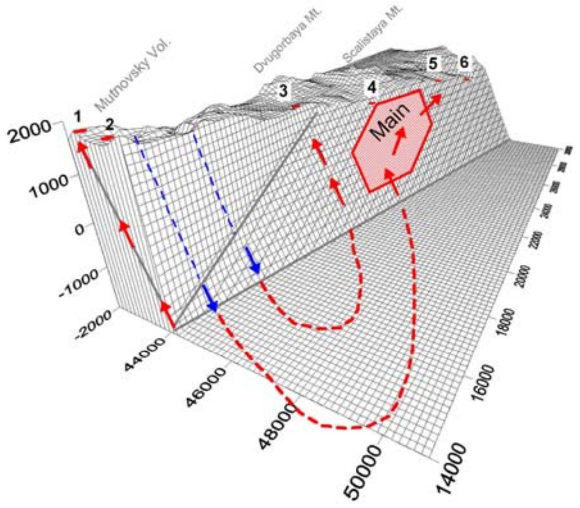

Figure. 1. Block-diagram of the North-Mutnovsky volcano-tectonic zone included the Main production zone plane. Possible streamlines of fluids from Mutnovsky volcano recharge area to Dachny and Verkhne-Zhirovskoy discharge areas through deeper part of zone, where heat and mass magmatic component exchange took place – are shown by arrows and dashed lines. Main production reservoir shown as polygon area. Steam discharge areas: 1 – Active crater of Mutnovsky volcano, 2 – Bottom Field of Mutnovsky volcano, 3 – North Mutnovsky (West), 4 – Dachny; Hot water discharge areas: 5 – Piratovsky, 6 – Verkhne-Zhirovsky.

Concepual hydrogeological model of the Dachny site of the Mutnovsky geothermal field shown in Figs.1 and 2. The Main production zone occur within North-Mutnovsky volcano-tectonic zone. Main production zone strikes north-north-east with east-east-south dip 60^o, and average vertical thickness 240 m. The Main production zone in Dachny site is penetrated by wells 045, 01, 014, 016, 1, 029W, 26, 24, 4E (Fig.2). The strike of production zone is subparallel to the system of the active faults (V.L. Leonov, 1986) (Fig. 3). Host rocks of production zone are: diorites, Miocene-pliocene sandstones, rhyolite and andesite tuffs and lavas. Nevertheless there is no explicit lithologic control of the production zone. Roof of the production zone is identified by circulation losses during drilling along the plane of Main production zone. Tracer tests interaction is also preferable along the Main production zone strike. The plane of the

Main production zone is intersect the active magma feeding chamber of Mutnovsky volcano at elevations of +250 - +1250 m.a..s.l. at the distance 8 km apart from production site (Fig.1). The Mutnovsky volcano crater glacier act as a meteoric water recharge area for the fluids producing by exploitation wells in the Dachny. Meteoric recharge accelerated and maintained by melting of the glacier due to high heat flows in the crater (Bottom Field, Fig.1). Heat feeding of the production zone is connected to magmatic bodies accumulated in the North Mutnovsky volcano-tectonic zone, but this is not clear weather or not those bodies are directly connected to magmatic system of the active Mutnovsky volcano, or just isolated remains of magma intruded in the hydrofracturing plane created by Mutnovsky volcano. Upflow of the high temperature fluids occur in the south-east part of the Main production zone, where liquid dominated conditions at 300^{o}C occurs (Fig. 2). Ascending fluids transfer to two-phase conditions in the shallow parts of the production zone (above 0 m.a..s.l.), where production zone traced by wairakite-chlorite secondary minerals association. Main production zone is also detected by Cl/SO4>1 ratios, and high values of Na-K geothermometer. Four additional wells (A1-A4), recently drilled (2001-2003) outside of the Main production zone were found to be non-productive. Steam explosion (June 2003) in 300 m east from well O45 (Fig.2) triggering by the exploitation looks as a pointer to the upflow root. Following are details of some specific points of the conceptual model above.

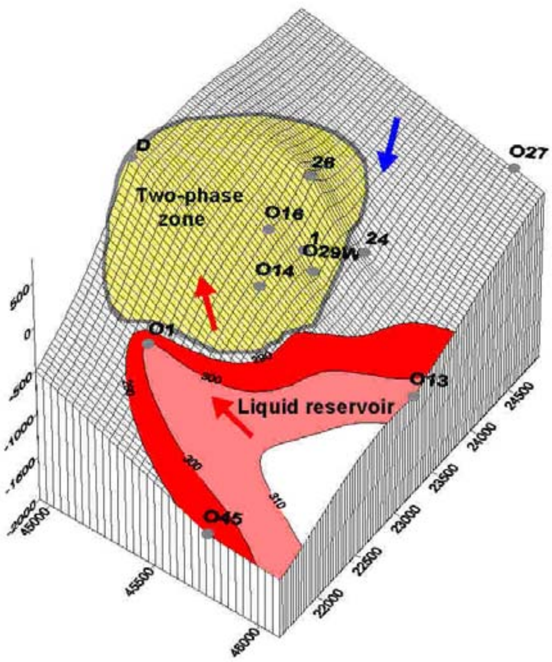

Figure. 2. Main production zone plane with temperature, phase distributions and production zones locations with corresponding well numbers.

2.1 Production and Circulation Loss Zones Distribution

The strike of production zone is subparallel to the system of faults (the so-called Vstrechny, Thermal, Pologiy, Tuffaceous and Krainiy), (V.L. Leonov, 1986) (Fig. 3). Roof and bottom elevations of the production zone are estimated based on S.G. Assaulov's data (1996) in which the roof elevation is estimated from the minimum depth of the production zone penetrated by slotted line.

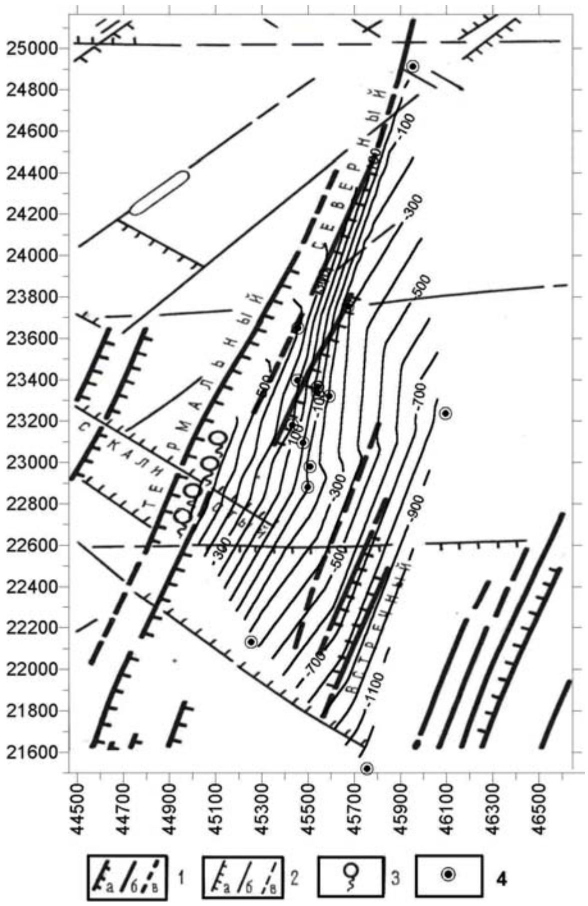

Fig. 3. Structural map of the Dachny site (V.L.Leonov, 1986) and top surface of the Main production zone (isolines): 1 – active fractures (north-north-east strike): a – with vertical displacements, б – without vertical displacements, в - assumed; 2- fractures of other strike: a – with vertical displacements, б – without vertical displacements, в - assumed; 3 – thermal manifestations, 4 – points of the production zone intersected by wells (Fig.2, Table 1).

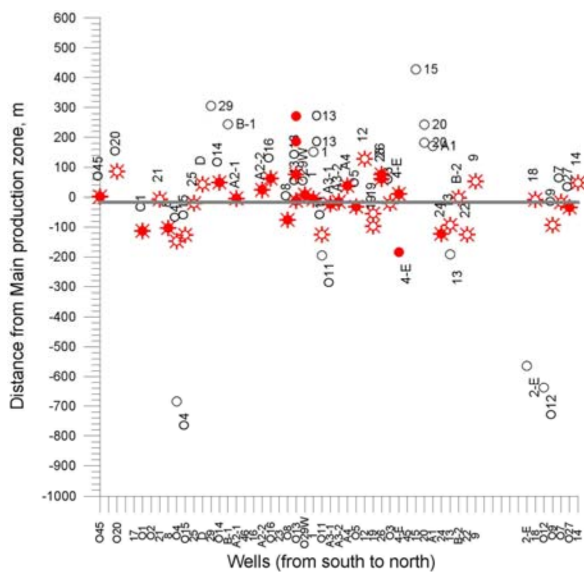

Figure. 4. Deviation from Main production zone plane (dz*cos(60.4^{o})): Z = -1.691076246561*X +0.48880109651512*Y +65583.1 to the points of the production (🗁☒) and full circulation loss (☰🗁) zones. Filled symbols correspond to production wells.

Fig.4 shows space deviation of the points of the full circulation loss from the Main production zone plane. 75% of all full circulation loss zones and 100% of all production wells are occur to ±150m thick interval of the Main production zone plane.

Another minor permeability zone may occur in the lower full circulation loss zones of the wells 04, 2E, 012, 4E and 011 within diorite intrusion contact, penetrated by wells below the Main production zone (Fig.4).

Table 1. Input data for mapping of the Main production zone in Dachny site (Fig.2 and Fig.3).

Well #	X	Y	Z	Roof of the Main zone m.a.s.l.	Vertical thickness, m
1	45540	23336	786	-34	280
26	45455	23650	816	428	78
O16	45432	23181	788	211	255
O27	45953	24912	813	-3	191
O29W	45591	23320	791	-219	63
O1	45254	22131	803	-353	39
O14	45499	22881	775	-96	142
O13	46095	23236	802	-858	291
O45	45756	21522	710	-1269	101
24	45673	23754	793	-288	219
Dachny steam jets	44950	22750	775	775	
A2-1	45509	22980	776.8	-151	
A2-2	45477	23096	776.8	15	210
A3-1	45539	23363	785	-52	
A3-2	45543	23365	785	-43	240
A4	45453	23398	780	232	90

2.2 Lithology and Geophysical Properties

There is no explicit lithological control of the production zones and circulation losses in the Dachny. Geological cross-section combined with permeability distribution data (Fig.5) shows Main production zone intersect all principal lithological units: quaternary ignimbrites, tuffs and lavas, acid magmatic extrusions; Pliocene lavas (Nal_2); Pliocene rhyolite tuffs (Nal_1); Miocene tuffs and lavas ($N_1^2as_2$); Miocene sandstones ($N_1^2as_1$); Miocene intrusion contact zone (N_1br); diorite intrusions (δN_1^2). Additional possibility of production zone may occur within contact zones and diorites bodies δN_1^2 (Fig.4: wells 04, 011, 012). Miocene/Pliocene structural surface (roof of the $N_1^2as_2$ unit) may also yield additional permeability to reservoir.

Geophysical properties are not clearly define reservoir characteristics. Units (Nal_1 ,$N_1^2as_2$, $N_1^2as_1$, N_1br, δN_1^2) are characterized by high γ-activity values (5.5 -9.8 mkR/hr), while units (Q_1, Nal_2) are varies in the range of (3.2 - 4.5 mkR/hr). No correlation between e-conductivity and lythological units were found. Production intervals are characterized by 30-100 Ohm*m resistivity values (wells 01, 013, 049N, 055), while low resistivity zones (1-10 Ohm*m) are not necessary coincide with productivity. Combined analysis of the lithological units and geophysical parameters (wells 04, 011, 012) show that diorites (δN_1^2) representing a combination of the dykes and magmatic bodies (with vertical thickness up to 150 m) are hosted by Miocene sandstones ($N_1^2as_1$).

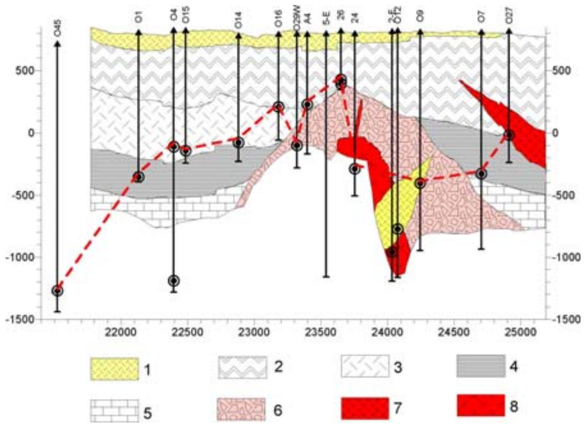

Fig. 5. Geological cross-section along line of wells 17-030 (G.M. Asaulov et al, 1987), combined with distribution of production zones/circulation losses (shown by filled circles) along wells 045-027. Main production zone trace shown by thick dashed line. All data projected on meridional axis. Lithological units: 1 – quaternary ignimbrites, tuffs and lavas, acid magmatic extrusions; 2 – Pliocene lavas (Nal_2); 3 – Pliocene rhyolite tuffs (Nal_1); 4 – Miocene tuffs and lavas ($N_1^2as_2$); 5 – Miocene sandstones ($N_1^2as_1$); 6 – Miocene intrusion contact zone (N_1br); 7,8 – diorite intrusions (δN_1^2).

2.4 Gas and Fluid Chemistry

The Main production zone penetrated by high well head pressure wells (working WHP>12 bars) characterized by Cl/SO4>1, high Na-K geothermometer values (compare to direct temperature measurements) and submeridional tracer interaction. In opposite to this downflows are characterized by low WHP wells, and low Cl/SO4<1 ratios. Cl/SO_4 ratio may be used for tracing of the roots of ascending flows in reservoir (fluid transport directed from high to low Cl/SO_4 ratios): 045→01→014→1→24→4E→5E and 013→029W→1→ 24→4E→5E (Fig.2, Table 3).

Table 2. Gas composition of the Dachny site exploitation wells (weight % in steam phase).

Well	CO_2	H_2S	He	H_2	Ar	N_2	CH_4	Gas content, weight %	Separation pressure, bars
Flow tests 1999 - 2000									
029W	77.4	21.0	0.0000	0.10	0.03	1.5	0.04	0.010	8.2
26	83.8	11.3	0.0000	0.20	0.10	4.4	0.17	0.108	7.3
016	87.0	10.7	0.0000	0.21	0.07	1.9	0.12	0.164	7.5
4E	87.5	9.00	0.0001	0.02	0.11	3.3	0.03	0.030	7.5
Exploitation, August 2003									
029W	87.8	9.74	0.0000	0.02	0.09	2.2	0.16	0.036	6.0
26	83.6	7.33	0.0000	0.50	0.21	7.7	0.67	0.037	6.0
016	92.1	4.4	0.0000	0.26	0.06	2.7	0.42	0.118	6.0
4E	94.3	4.12	0.0001	0.01	0.07	1.4	0.07	0.045	6.0
5E	89.4	7.26	0.0001	0.02	0.10	3.2	0.04	0.067	6.0

Gas and fluid chemistry variations response to exploitation are valuable for reservoir state and boundary conditions assessment. It was observed (Table 2) increase of the N_2 fraction and decrease of the H_2S (wells O16, O29W and 26) which may reflect the meteoric water inflows in reservoir. This coincide with the Na/K geothermometer decline observations (20^{o}C in well 4E, 4.5^{o}C for well O29W) (Table 3).

Table 3. Production and chemistry characteristics of wells in Dachny site depending on type of reservoir fluid conditions.

Well	Date	Rate, kg/s	Enthalpy kJ/kg	WHP max bars	T Na-K °C	Cl/SO_4
Main upflow						
O45	1991	21	2320	20.1	291	4.83
O1	1988	53.2	1500	21.9	303	3.06
O13	1988	44.8	1278	13.5	303	1.70
029W	2000	71	1150	18.4	268	2.30
029W	2003	72.5	1181		245	1.64
029W	2003				264	1.53
O14	1988	8.4	2050	35.8	266	1.31
1	1988	20	1450	14.6	276	1.25
24	1988	35	1204		275	1.1
Condensate downflow						
O12	1987			7.1	240	0.70
O3	1987			3.9	262	1.00
O11	1987			3.6	228-276	0.30
4E	1999	26.9	1200	11.8	274	0.98
4E	2001	32.8	1104	8.9	277	1.08
4E	2003				251	0.95
5E	2002	36.9	1097	11.7	252	0.78
5E	2003				267	0.71
5E	2003				249	0.74

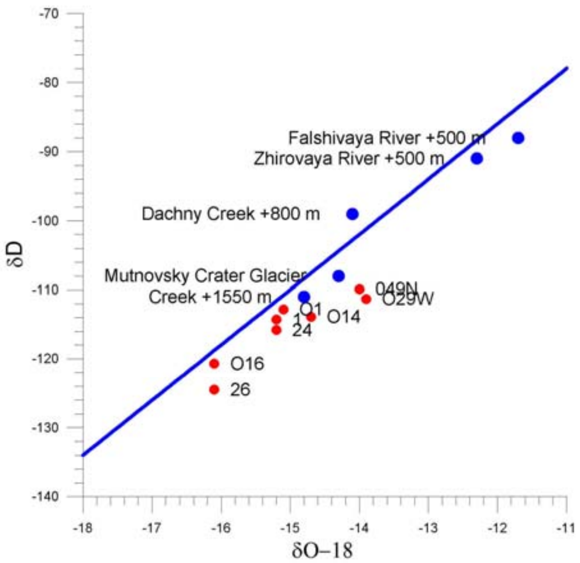

Fig. 6. Hydroisotope composition of the fluids from Mutnovsky exploitation wells and local meteoric waters (Kiryukhin et al, 2000, 2002).

Exploitation wells (O29W, 1, 24, 4E, O14, O49N) hydro isotope values are corresponding to the meteoric water recharge area at +1500 - +1600 m.a.s.l. (Fig.6), where Mutnovsky volcano glacier melting due to high heat flows in the crater (Bottom Field, Fig.1). More light hydro isotope values of the steam wells 016 and 26 (Fig.6) resulted from isotope fractionation in shallow two-phase reservoir conditions.

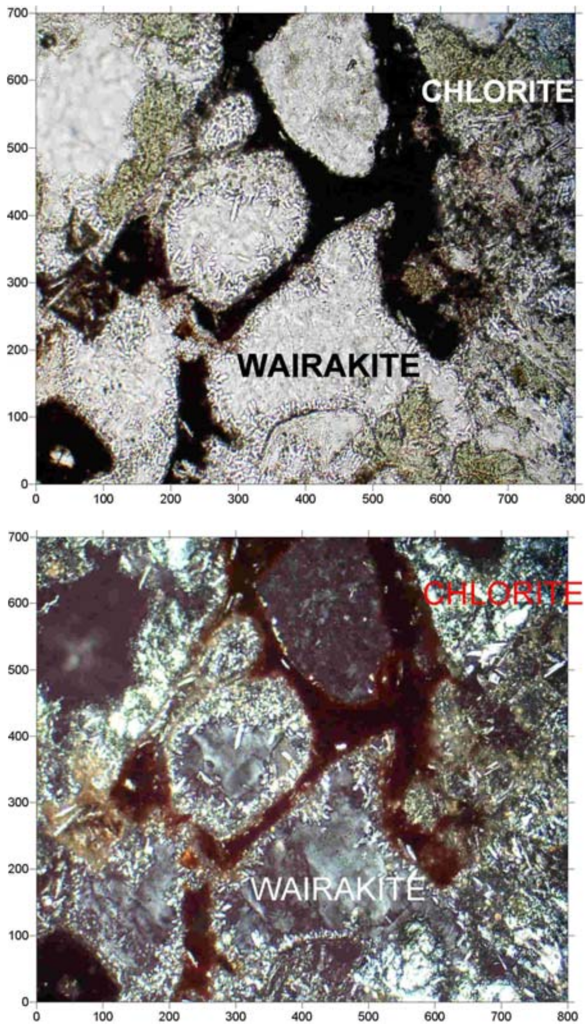

Fig.7. Photos of thins from samples ejected from well A3 during penetration of the Main production zone at depth 894 m. Upper photo - analysator off, lower photo – nikoles ×. Lower photo shows polysynthetic twins of wairakite. Scale in mkm. Photo from M.Y. Puzankov, 2003.

2.5 Secondary Mineralization

The following secondary minerals associations were detected in the Dachny site (Slovtsov, 2001): (1) Quartz-epidote-chlorite association characterized by Na-Cl fluids circulation at temperatures of 220-300°C, (2) Wairakite-prehnite-quartz association with two-phase conditions at 150-240°C (pressures 5-35 bars), (3) Illite-chlorite-calcite zone, corresponding to condensate downflows of SO_4-Cl-HCO_3 composition at 150-220°C. Rock samples ejected from recently drilled wells A2-A4 during events of the Main production zone penetration shows wairakite-chlorite as a dominant secondary minerals association (Fig.7), while there was no wairakite found outside of the production zone.

2.6 Recent Drilling Results

Four additional wells (A1-A4) recently drilled (2001-2002) and equipped with slotted liners outside of the Main production zone has demonstrated zero or low productivity. Regretably, A1 was directed outside of the Main production zone, wells A2 and A3 penetrated Main production zone (these events correspond to full circulation losses, up to 0.5 m drops of drill bits, and other drilling failures), nevertheless production intervals were cemented and isolated by casing. In both wells A2 and A3, the Main production zone was penetrated from 2-nd attempt, so additional directional branches were drilled in the same wells. After Main zone passed no any drilling problems observed (Rosly, 2003). Well A4 was drilled through Main production zone to deeper temperature inversion zone, where cold inflows quenched production.

2.7 Geothermal Analogs

The similar "single fault" type geothermal fields have been found in Japan (Ogiri) where 30 MWe comes from single fault of 20 m thick and 232°C liquid phase circulates in andesite host rock (Goko, 2000). Similar examples are Okuaizu (Japan) (Mizugaki, 2000) and Dixie Valley (USA) (Bodvarsson, 2000).

3. MODELING OF THE NATURAL STATE CONDITIONS AND EXPLOITATION OF DACHNY SITE IN THE MUTNOVSKY GEOTHERMAL FIELD

3.1 The numerical model description

3.1.1 Grid

Grid generation based on AMESH preprocessor (1999), which yield TOUGH2 input parameters in terms of horizontal connections parameters d1, d2, AREA. Then additional correction procedure was implemented to specify vertical component in grid connection (Fig.8). In addition to this, the more accurate BETAX presentation (format F20.14 instead of F10.4) used to avoid "parasitic circulation" in the model (according to K. Pruess, pers. com., 1998).

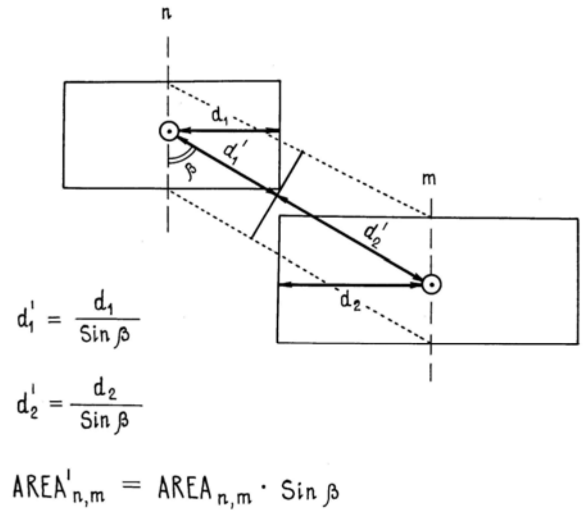

Figure. 8. Mesh parameters (d1, d2, AREA) corrections applied to A-MESH output.

Geothermal reservoir is represented as a combination of two layer-type reservoirs: A-reservoir and B-reservoir. A-reservoir numerical grid corresponds to the Main production zone with averaged vertical thickness 240 m (actuaaaal thickness 120 m), each element of which is located at the specified elevation corresponding to the Main production zone (Figs.9 and 10). B-reservoir numerical grid includes three elements corresponding to wells 2E, 5E and O12 diorite intrusion contact permeability zones. In total 24 existing wells, 39 additional interior elements (F-elements and D-element) and 12 boundary (inactive) elements (B-elements) are specified in the model.

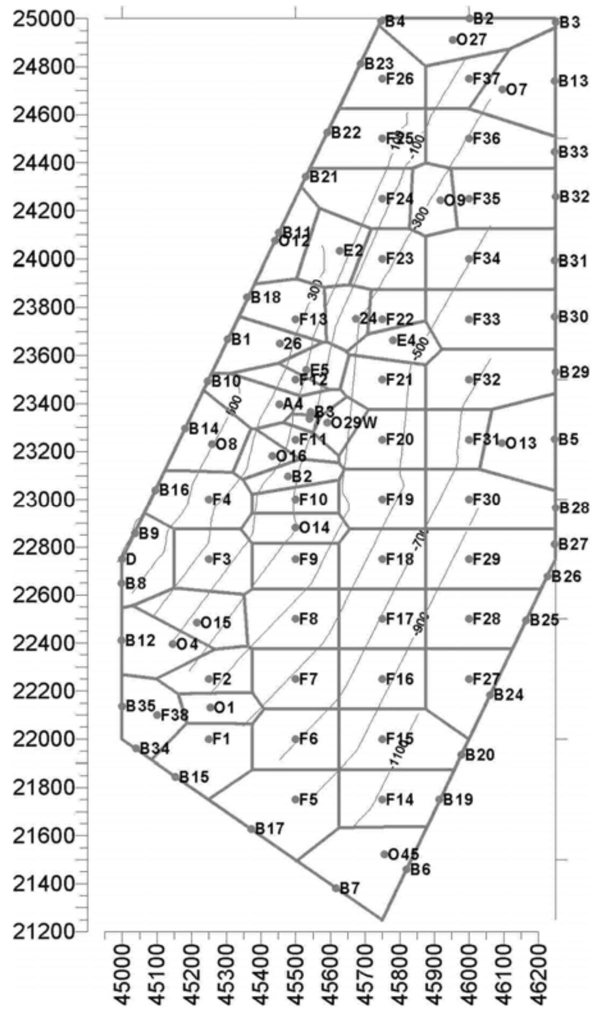

Figure. 9. Dachny site in the Mutnovsky geothermal field. Numerical grid of the A-reservoir elements and its elevations (m.a.s.l.).

3.1.2 Sinks/Sources, Permeability Distribution and Boundary Conditions

Figs.10 and 11 demonstrates grid and permeability distributions assigned in the A-reservoir and B-reservoir of the model. «Sources» in the model are O45, F27, F28, F14, F15, F29, permeability and rock properties are assigned based on the previous modeling (1996, 2002) and then they are corrected taking into account the natural state condition modeling results. Boundary conditions are assigned in B-elements as P=const and T=const (natural state modeling). Heat exchange between the model elements and host rock with average temperature 90°C are specified through QLOSS subroutine where heat exchange coefficient is assigned as 0.0042 W/m^2 °C.

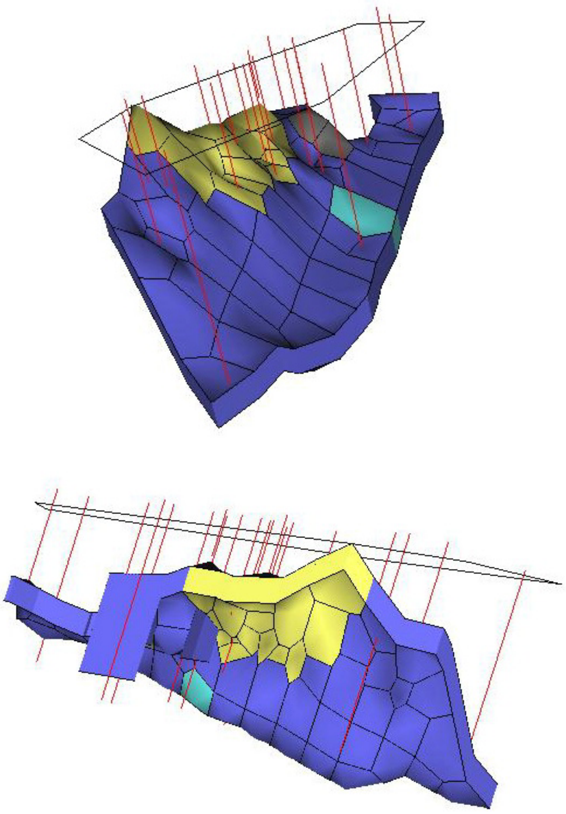

Figure. 10. Geometry of the 3-D numerical model of the of the Dachny site. Upper figure: view from above south-east, lower figure: view from below south-west. Colors correspond to different permeability domains (Fig.11).

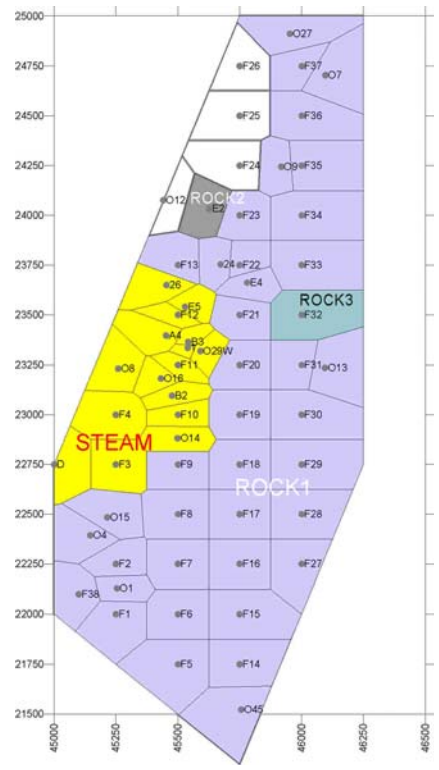

Figure. 11. Permeability distribution in the A-reservoir (Main production zone) STEAM, ROCK1, ROCK2 and ROCK3 domains with 100 mD, 100 mD, 1 mD and 0.01 mD, correspondingly.

3.2 Natural State Modeling

Natural state modeling is targeted to temperature, pressure and phase condition match in the key elements (Table 4) to improve model sources and sink parameters, and permeability distribution. Based on above, total upflow rate estimated in the model is 54 kg/s, with mass rates and enthalpies specified as 9 kg/s and 1390 кJ/кg (water 307^{o}C) in each "source" element (3.1.2). Permeability distributions in A-reservoir domains STEAM, ROCK1, ROCK2 and ROCK3 are estimated as 100 mD, 100 mD, 1 mD and 0.01 mD correspondingly, in B-reservoir ROCK1 domain - 100 mD.

Table 4. Key elements for natural state model calibration. Notes: * -Na-K geothermometer, ** -CO_2-geothermometer, [$] -Custer P-logs, [&] -S.G. Assaulov et al 1996, [$$] -Capillary tubing system, Bold letters correspond to saturation pressures.

Well #	X	Y	Z	Roof of the Main zone m.a.s.l.	Vertical thickness, m
1	45540	23336	786	-34	280
26	45455	23650	816	428	78
O16	45432	23181	788	211	255
O27	45953	24912	813	-3	191
O29W	45591	23320	791	-219	63
O1	45254	22131	803	-353	39
O14	45499	22881	775	-96	142
O13	46095	23236	802	-858	291
O45	45756	21522	710	-1269	101
24	45673	23754	793	-288	219
Dachny steam jets	44950	22750	775	775	
A2-1	45509	22980	776.8	-151	
A2-2	45477	23096	776.8	15	210
A3-1	45539	23363	785	-52	
A3-2	45543	23365	785	-43	240
A4	45453	23398	780	232	90

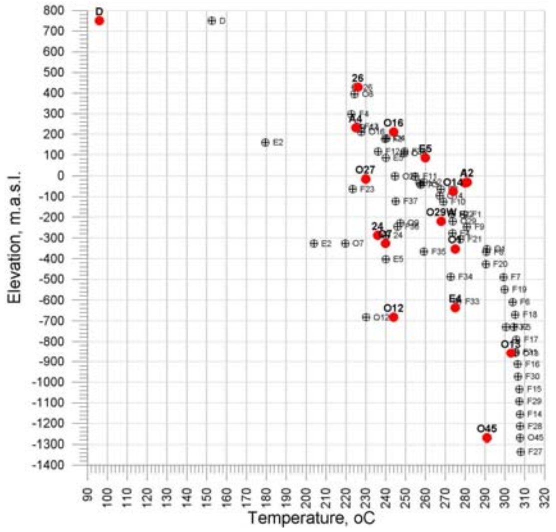

Fig.13a. Modeling natural state conditions (temperature match): key elements data (filled circles), model data (empty circles).

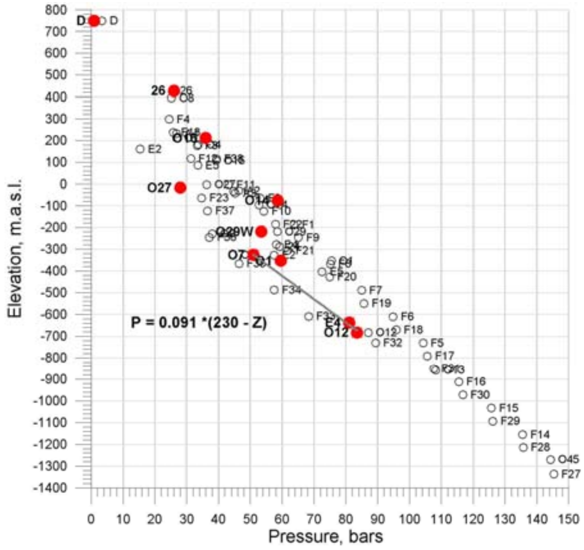

Fig.13b. Modeling natural state conditions (pressure match): key elements data (filled circles), model data (empty circles).

Figs.13 shows corresponding temperature and pressure match in the key elements in vertical projection of the model. Upflow (wells O45-O13-O29W-O16-26-D) and downflow (wells O27-O7-4E-012) patterns are clearly defined in the pressure vertical distributions profiles.

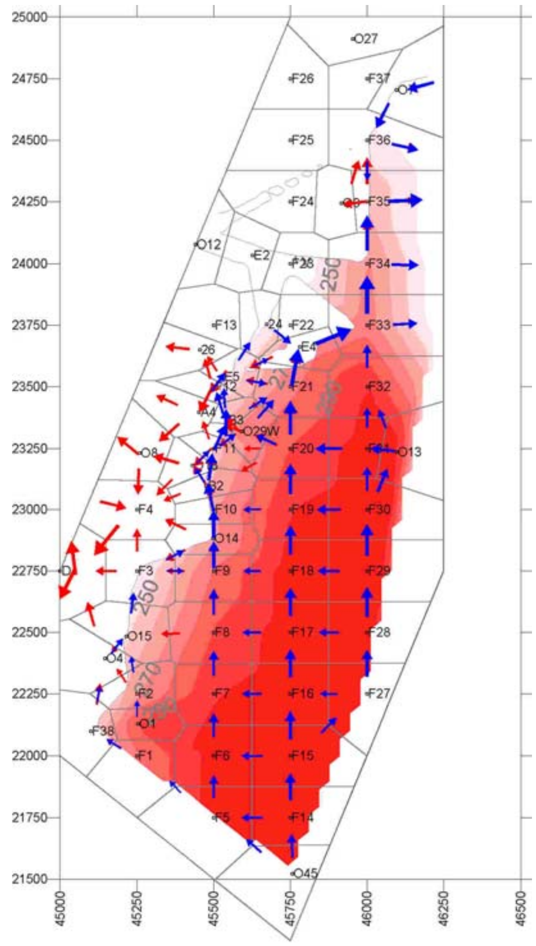

Fig.14. Modeling natural state conditions: temperature distribution in liquid dominated zone (where steam saturation less than 0.08), flows are shown by arrows - steam (red) and liquid (blue), in proportional scale.

Fig.14 shows temperature, steam saturation and flows distribution within the Main production zone (liquid flows are greater than 1 kg/s and steam flows are greater than 0.1 kg/s between the elements). Upflows are directed from south-east part to north-north-east part (liquid discharge) and west part (steam discharge, element D – the so-called Kotel) of the production zone.

4.MODELING OF THE EXPLOITATION

4.1 Input data for the model and calibration

Model calibration is based mainly on the data received from initial production tests of wells 016, 26, 029W, 4Э, A2 and 5E, and data of the total steam and total separate production from Mutnovsky PP separator. The total steam production (at 6 bars abs) of the above mentioned wells declined from 64.9 kg/s to 59.4 kg/s (8.5%), the total separate production declined from 117.5 kg/s to 107.5 kg/s (8.5%) during one year exploitation period (Figs. 15 and 16). Pressure monitoring well O12 shows 0.75 bar pressure drop during one-year exploitation period, but this data does not characterize production zone where exploitation took place.

At this stage of calibration the compressibility coefficient was found necessary to be implemented in the model: 5.0 10^{-7} Pa^{-1} in STEAM domain and 5.0 10^{-8} Pa^{-1} in the rest domains.

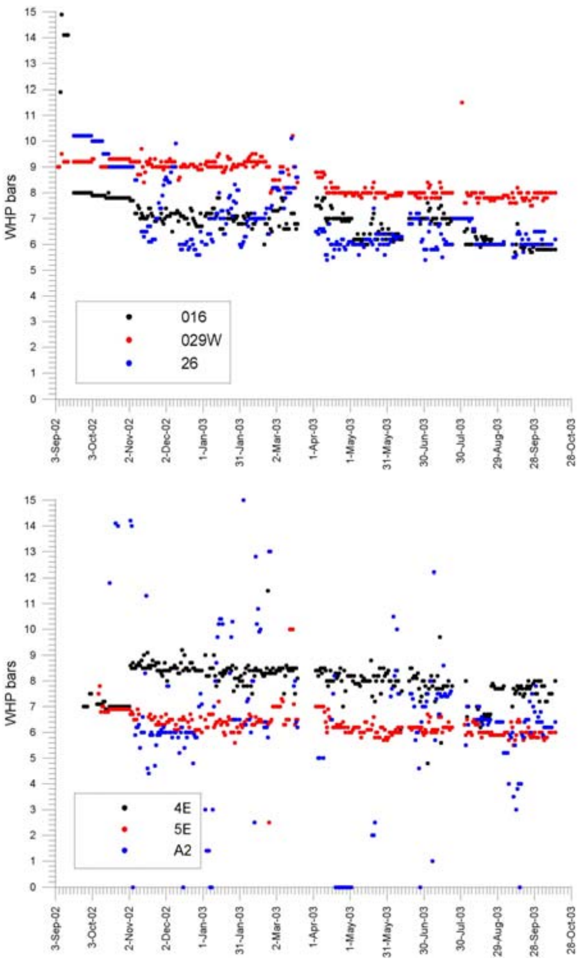

Fig.15. Well Head Pressure (WHP, bars) variations) in exploitation wells of the Dachny site Mutnovsky geothermal field during 1-st year of the exploitation (AO "Geotherm", 2003).

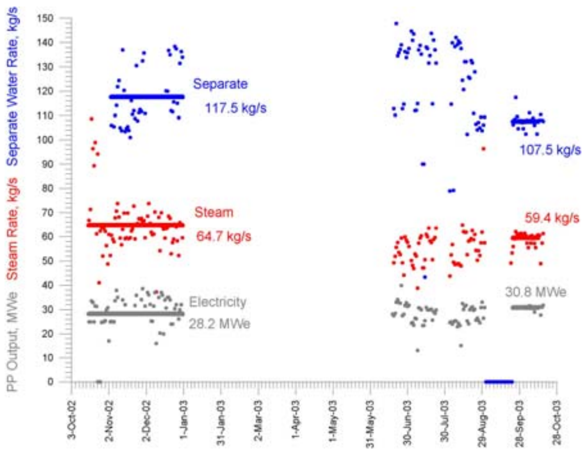

Fig.16. Mutnovsky PP electricity output and total steam and separate water production at PP separator at 6 bars (AO "Geotherm", 2003).

4.2 Modeling of well-reservoir interaction

TOUGH2V2.0 coupled wellbore flow option used. For this purposes the total productivity indexes were split in the following way:

$$PI = (k_{rs}\rho_s / \mu_s + k_{rw}\rho_w / \mu_w)\, PI_0$$

- where $k_{r\beta}$ - relative phase permeability, μ_β - viscosity Pa*s, ρ_β - density, kg/m^3, PI_0 – productivity indexes (m^3) (liquid (β=w) or steam (β=s)). Productivity indexes PI_0 of five production wells estimated accordingly to wells rates (Q) and wells head pressures (WHP) (corresponding to initial exploitation data), flowing enthalpies h, reservoir P_r and bottomhole P_b pressures, and relative permeabilities (k_{rs}, k_{rw}) derived from the model (TOUGH2 and HOLA) (Table 5). Grant type relative permeabilities used.

Table. 5 Exploitation wells O16, 26, E4, O29W, E5 and additional F-wells parameters used for productivity indexes estimation.

Well	Q kg/s	WHP bar	h kJ/kg	P_b bar	P_r bar	PI kg/s bar	PI_0 m^3
O16	17	7.5	2400	13.9	21.6	2.2	2.52 10^{-11}
26	18	7.5	2800	13.7	25.5	1.5	1.97 10^{-11}
4E	26.7	9	1338	24.9	58.2	0.8	1.37 10^{-12}
029W	72.5	9	1216	50.4	58.4	9.1	1.20 10^{-11}
5E	39	7	1072	27	33.5	6.0	9.22 10^{-12}
F-wells		7				1.0	1.30 10^{-12}

Bottom hole pressure P_b(WHP, Q, h, d) is calculated in the form of electronic tables based on HOLA code (Fig. 17). Fig.17 shows that enthalpy decline below 1100 kJ/kg may turns off a two-phase production wells (well O29W, for example). In addition steam saturation increase may cause 3.3 times total productivity index decrease at 300^{o}C, that quenches wells in case of extensive boiling in reservoir. Steam well production is less sensitive to reservoir enthalpy variations.

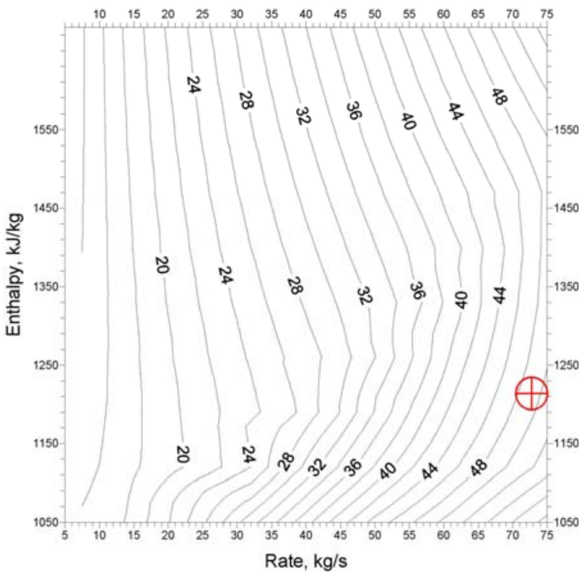

Figure. 17. Bottom hole pressures in well O29W vs mass flowrate and enthalpy under WHP 9.0 bar. Symbol ⊕ means initial well parameters.

4.3 Modeling of Dachny site exploitation in the Mutnovsky geothermal field up to 2012 year

<u>4.3.1 Modeling of 016, 26, 029W, E4 and E5 exploitation</u>

Exploitation wells are assigned under well head pressure conditions corresponding to the data from Table 1, well 027 is specified at reinjection with mass rate 84 kg/s and enthalpy 700 kJ/kg. Two scenarios of exploitation up to 2012 year are studied: (#1) Five wells 016, 26, 029W, E4 and E5 exploitation, (#2) The same as #1, plus two times (x2) exploitation load increase in the model elements 016, 26, 029W, E4 and E5.

The switch to "no flow" boundary conditions during exploitation implemented in B1, B10, B14, B16, B9, B8 boundary elements in the model. Two-phase wells were switched off if mass flowrate dropped less than 5 kg/s, steam wells were switched off if mass flowrate dropped below 2 kg/s.

Modeling results for two scenarios are represented in Figs. 18 and 19. Scenario #1 (Fig. 18) shows total steam production drop of the wells 016, 26, 029W, E4 и E5 from 64 to 33 kg/s during the 10 year exploitation period, and 13 bars pressure drop in reservoir (A3 element). Scenario #2 (Fig. 19) shows total steam production drop of the wells from 130 to 40 kg/s during the 10 year exploitation period, and 18 bars pressure drop in reservoir (A3 element). Wells 26 and 5E may be abandoned by 4-th and 5-th year of exploitation, correspondingly.

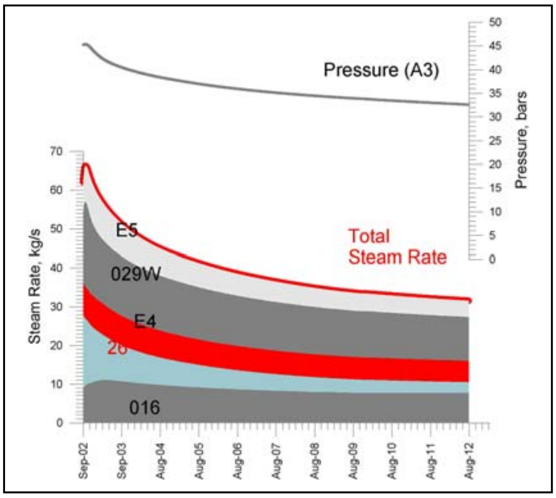

Figure. 18. Scenario #1: modeling of the steam production at 7 bars (wells 016, 26, E4, 029W, E5) and reservoir pressure (A3 model element) response in the Dachny site.

4.3.2 Modeling of the additional F-wells load exploitation scenario (#3)

Mutnovsky 50 MWe PP needs 95 kg/s of 7 bars steam in stable terms during exploitation period. Additional study of the steam productivity yield (from model elements F16, F17, F18, F19, F20, F29 and F30) was performed. Corresponding F-wells locations and constructions are shown in Fig.20 and Table 6. F-wells targeted to the high temperature upflow zone in the south-eastern part of the Main production zone. All F-wells suggested to be deviated wells drilled from positions of existing wells O13 and O10 correspondingly (Fig. 20), until first full circulation loss after depth mentioned in Table 6. Bottomhole pressures tables calculations based on HOLA code. Wellbore diameter 0.246 m until depth 900 m, and then 0.168 m assumed.

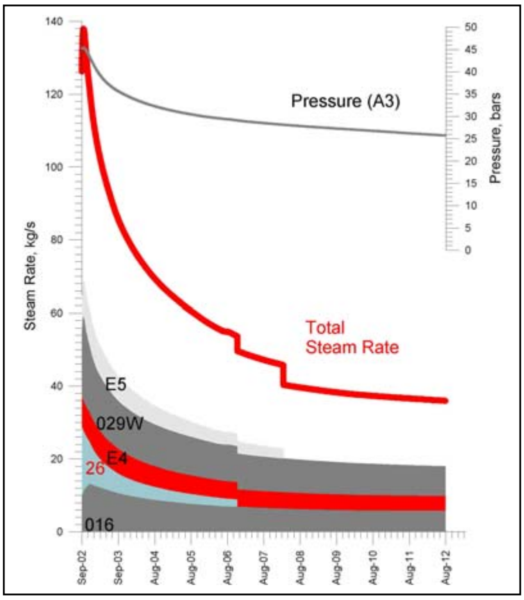

Figure. 19. Scenario #2: modeling of the steam production at 7 bars (doubling load of the wells 016, 26, E4, 029W, E5) and reservoir pressure (A3 model element) response in the Dachny site.

Table 6. F-wells parameters.

F-wells	Depth, m	Horizontal deviation, m	Angle of vertical deviation
O13-F30	1792	254	8.2
O10-F16	1901	795	24.7
O10-F17	1755	709	23.8
O13-F18	1588	596	22.1
O13-F19	1414	418	17.2
O13-F20	1277	345	15.7
O10-F29	1963	461	13.6

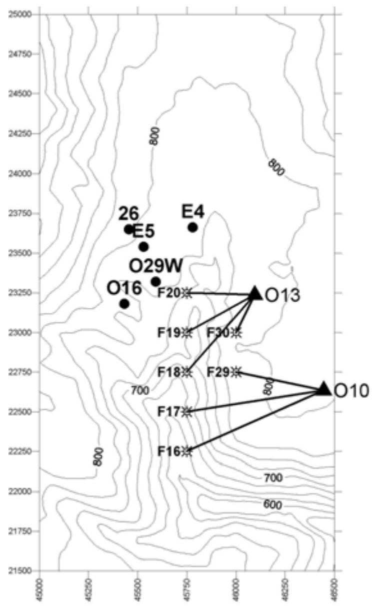

Figure. 20. Existing operating wells: solid circles. Additional F-wells: drilling targets (stars) and drilling rig positions (triangles).

Exploitation load was assigned accordingly to #1 scenario plus additional seven wells were subsequently add to match 50 MWe PP demand during 10 years exploitation period. All additional exploitation F-wells were assign at 7 bars WHP and with 1.3 10^{-12} m^3 productivity indexes (Table 5).

Modeling results for #3 scenario are represented in Figs. 21. Total steam production of the wells ranges from 77 to 111 kg/s (7 bars) during the 10-year exploitation period (95.1 kg/s in average), and 19.8 bars pressure drop observed in reservoir (A3 element).

Additional modeling study shows that reinjection of separate from F-wells in F27 and F28 model elements doesn't yield significant effect on steam production.

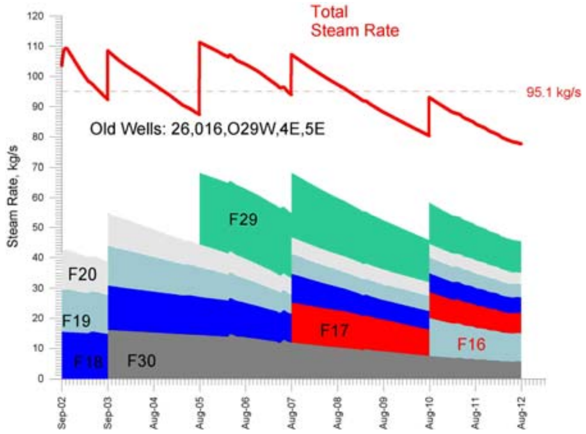

Figure. 21. Scenario #3: modeling of the steam production (old wells: 016, 26, E4, 029W, E5 and additional F-wells) in the Dachny site.

4.3.3 Modeling of the additional FA-wells load exploitation scenario (#4)

It was requested from AO "Geotherm" to make also another modeling considerations of the drill rig locations, though to minimize steam transportation line distances from wells to PP (Fig.22, Table 7). Note drilling from the west bank of Falshivaya river may be more difficult compare to F-wells drilling from east bank, because of small angles between drilling direction and the Main production zone plane. Nevertheless, additional study of the steam production yield (from model elements F7, F8, F9, F17, F18, F19 and F20) was performed. Corresponding FA-wells locations and constructions are shown in Fig.22 and Table 7. FA-wells targeted to the high temperature upflow zone in the south-eastern part of the Main production zone. All FA-wells suggested to be deviated wells drilled from positions of existing well O14. Bottomhole pressures tables calculations based on HOLA code, wellbore diameter 0.246 m until depth 900 m, and then 0.168 m assumed.

Exploitation load was assigned accordingly to #1 scenario plus additional seven wells were subsequently add to match 50 MWe PP demand during 10 years exploitation period. All additional exploitation FA-wells were assign at 7 bars WHP and with 1.3 10^{-12} m^3 productivity indexes. Modeling results for #4 scenario are represented in Figs. 23. Total steam production of the wells ranges from 69 to 108 kg/s (7 bars) during the 10-year exploitation period (82.7 kg/s in average), and 22.7 bars pressure drop observed in reservoir (A3 element).

Table 7. FA-wells parameters

FA-wells	Depth, m	Horizontal deviation, m	Angle of vertical deviation
O14-F9	984	131	7.7
O14-F8	1188	381	18.7
O14-F7	1423	631	26.3
O14-F18	1472	283	11.1
O14-F19	1353	278	11.9
O14-F20	1282	446	20.4
O14-F17	1631	456	16.3

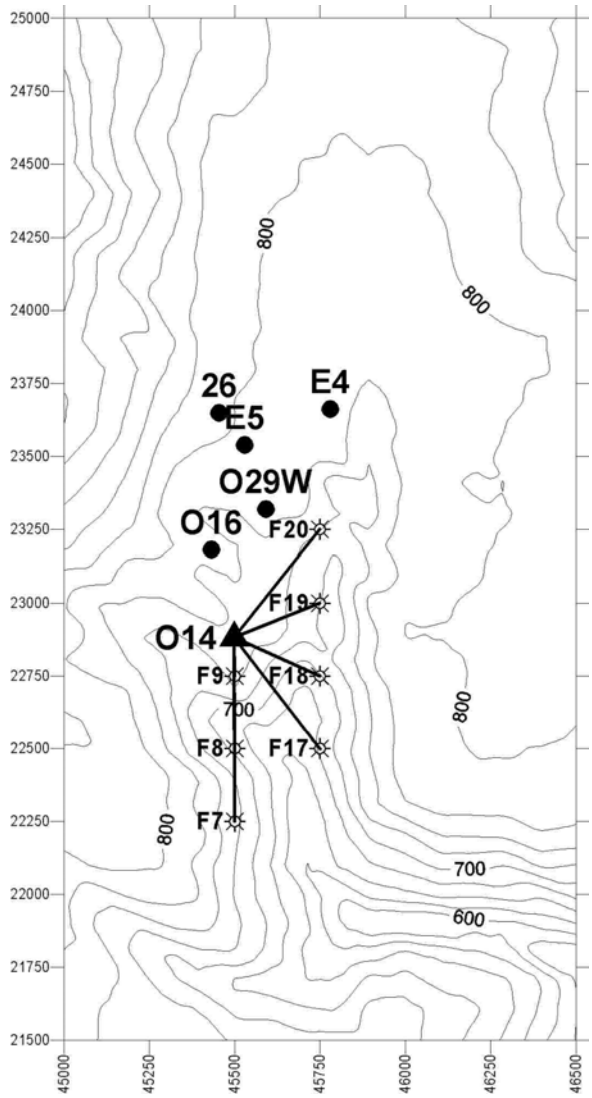

Figure. 22. Existing operating wells: solid circles. Additional FA-wells: drilling targets (stars) and drilling rig positions (triangles).

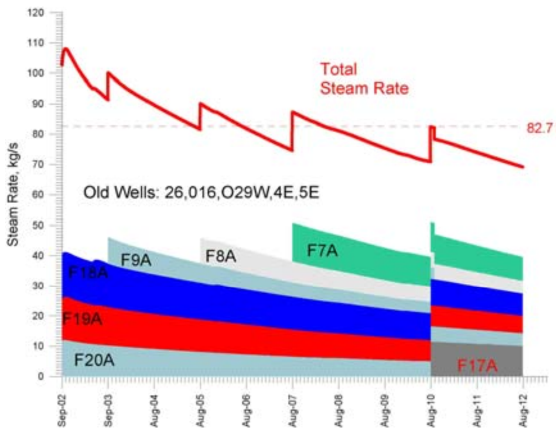

Figure. 23. Scenario #4: modeling of the steam production (old wells: 016, 26, E4, 029W, E5 and additional FA-wells) in the Dachny site.

CONCLUSIONS

1. Conceptual hydrogeological model of the Dachny site Mutnovsky geothermal field was verified based on mapping of active fracture zones, circulation losses and production zones distribution data, gas and fluid chemistry data, secondary minerals distributions, recent results of drilling (4 wells) and geothermal analog data. Central part of the Dachny represent a "single fault" type geothermal reservoir with the Main production zone of 240 m vertical thickness, north-north-east strike and 60^o east-east-south dip. Upflow of the high temperature fluids occur in the south-east part of this zone, where liquid dominated conditions at 300^{o}C occurs. Ascending fluids transfer to two-phase conditions in the shallow parts of the production zone.

2.TOUGH2V2.0 based numerical model strongly related to the particular wells and Main production zone has been developed (A-Mesh grid generator with corrected vertical connections parameters, one parameter-specified heat exchange to host rocks). Numerical model calibrated on natural state matches and one year exploitation data. Possible exploitation scenarios were analyzed based on this model (see points 3. and 4. below).

3. Steam production at 7 bars from the existing production wells of the Dachny site in the Mutnovsky geothermal field (016, 26, E4, 029W, E5) is limited by 60-70 kg/s with possibility of decline down to 33 kg/s during the first 10 years of the exploitation. Significant exploitation load in central part of the Dachny site will not yield adequate steam production increase in stable terms, moreover, it may have negative effect for steam productivity.

4. Mutnovsky 50 MWe PP needs 95 kg/s of 7 bars steam in stable terms exploitation period. Modeling study of the steam production increase from the Dachny site show necessity of the additional drilling targeted to south-east portion of the Main production zone. There are two options for additional wells drilling: from east bank of Falshivaya river (F-wells, Fig.20) or from west bank (FA-wells, Fig.22). In both cases seven additional directional wells with depth range of 1277-1963 m (deviation angle up to 24.7^o) for F-wells scenario and 984-1631 m (26.3^o) for FA-wells scenario were specified in the model. F-wells scenario #3 show possibility of the 95.1 kg/s steam production in average terms during 10-year exploitation period. FA-wells scenario #4 show possibility of the 85.7 kg/s steam production in average terms during 10-year exploitation period.

5. The modeling results show necessity of reliable and regular (per month) enthalpy-flowrate data receipt from production wells under exploitation conditions. Chemistry and gas monitoring data obtained during exploitation may be useful to detect the boundary conditions. Reservoir pressure data in the central part of geothermal reservoir is desired too. All the above data are necessary for proper calibration of the numerical model and accurate forecast of steam production scenarios.

6. In terms of stable conditions of steam supply to 50 MWe Mutnovsky Power Plant the possibility to use Verkhne-Mutnovsky site located 1.5-2.5 km north-east from Dachny site should be analyzed. This study is on-going.

ACKNOWLEDGEMENTS

The author expresses gratitude to AO "Geoterm" staff: General Director V.E. Luzin, Department Chief V.M. Morgun, hydrogeologists I.I. Chernev and L.K. Moskalev for helpful discussion and data support; Kamchatka EMSD GS RAS staff scientist D.V. Droznin for computer graphics support. This work has been supported by AO "Geoterm" contract №30 of 16.04.2003, Russian Basic Sciences Foundation grant 03-05-65373 and Russia Ministry of Education Grant 02.01.023.

REFERENCES

G.M. Assaulov et al (1987) Report on exploration works on Dachny site Mutnovsky geothermal field and feasibility study of the 50 MWe PP (in 7 volumes), Termalny (in Russian).

Z.P.Aunzo, G.Bjornson, G.S.Bodvarsson (1991), Wellbore models GWELL, GWNACL, and HOLA.Users Guide // Draft,1991,81 p.

S.G. Assaulov, N.P. Assaulova Mutnovsky geothermal field, DATABASE 1996 (Copy presented to WestJEC for implementation of the Kamchatka Feasibility Study).

G. Bodvarsson Long-Term Monitoring of high- and low-enthalpy fields under exploitation: Modeling and Management of geothermal systems // WGC Short Cources. Japan, 2000 P. 77-96.

C. Haukwa (1999) AMESH A mesh creating program for the Integral Finite Difference Method // LBNL Users Manual, 54 p.

Feasibility Study of the Integrated Power and Heating Plant System Sustained by the Mutnovsky Geothermal Field in Kamchatka // West JEC, 1997 // Report for EBRD.

Geothermal and Geochemical Studies of High-Temperature Hydrothermal (Using the Pattern of the Mutnovsky Geothermal Field). Moscow, Science, 1986 , p. 305.

Goko, K., 2000. Structure and hydrology of the Ogiri field, West Kirishima geothermal area, Kyushu, Japan. Geothermics 29 (2), 127-149.

A.V. Kiryukhin, I. Delemen and D. Gusev. High-Temperature Hydrothermal Reservoirs, M. Science, 1991, p. 160.

A.V. Kiryukhin, 1992. Progress Report on Modeling Studies LBL-32729, p. 21.

A.V. Kiryukhin. High-Temperature Fluid Flows in the Mutnovsky Hydrothermal System, Kamchatka // Geothermics, v.23, No. 1, 1993, pp.49-64.

A.V. Kiryukhin. Modeling Studies: Dachny Geothermal Reservoir, Kamchatka, Russia // Geothermics, v.26, No.1, 1996, pp.63-90.

A.V. Kiryukhin, M. Takahashi, A. Polyakov, M. Lesnykh and O. Bataeva (1998) Studies of the Mutnovsky Geothermal Field Water Recharge Conditions with the Use of Data on Oxygen (O^{18}) and Hydrogen (D) Isotopy // Volcanology and Seismology, № 4-5, pp.54-62.

A.V. Kiryukhin, S.M. Fazlullin, A.Y. Polyakov et al // Report on contract #32 on Gas and Chemical Testing of wells 4E, 016 , 26 , 029W, 2000, 23 p.

A.V. Kiryukhin. Modeling of Exploitation of Geothermal Fields // Vladivostok, Dalnauka, 2002, p. 216.

A.V. Kiryukhin Modeling of the Exploitation of the Mutnovsky Geothermal Field in Connection to 50 MWe PP steam supply //PROCEEDINGS, Twenty-Ninth Workshop on Geothermal Reservoir Engineering Stanford University, Stanford, California, January 26-28, 2004, 8p.

A.V. Kiryukhin, V.L. Leonov, I.B. Slovtsov, I.F. Delemen, M.Y. Puzankov, A.Y. Polyakov, G.O. Ivanysko, O.P. Bataeva, M.E. Zelensky Modeling of the exploitation of the Dachny geothermal field in relation to steam supply to Mutnovsky PP// Volcanology and Seismology Journal , 2004, 50 p. (in Russian)

V.L. Leonov Structural Conditions of Localization of high temperature hydrotherms , Moscow, Nauka publ., 1989, 104 p. (in Russian).

Mizugaki K. Geologic structure and volcanic history of the Yanaizu-Nishiyama (Okuaizu) geothermal field, Northeast Japan // Geothermics. 2000. V. 29. № 2. P. 233-256.

K. Pruess (1987) TOUGH users guide .Lawerence Berkeley Lab. Report, LBL 20700, ,Berkeley, California, 78 p.

K. Pruess (1991) TOUGH2 - a general purpouse numerical simulator for multiphase fluid and heat flow, Lawerence Berkeley Lab. Report, LBL-29400, Berkeley, California, 102 p.

K.Pruess (1999) “TOUGH2 Users Guide, Version 2.0” // LBL-43134.

Rosly G.A., 2003. Main Results of Exploitation Drilling // Report on AO Geoterm Workshop, June, 2003, Petropavlovsk-Kamchatsky, 35 p.

Slovtsov I.B. Rock Alteration in the Mutnovsky Hydrothermal System, Kamchatka, Russia // WRI Symp., Italy, 2001. P. 4